

## 2. ACCELERATOR AUGMENTATION

### 2.1 HIGH CURRENT INJECTOR

#### 2.1.1 Introduction

High Current Injector (HCI) is an upcoming Heavy Ion Beam Accelerator Facility at IUAC, New Delhi. It is designed to produce energetic ions of 1.8 MeV/u having mass to charge ratio ( $A/q$ )  $\leq 6$  and will be an injector to the existing Superconducting (SC) Linear Accelerator (SC-LINAC). We have achieved a major milestone in the project in this academic year with the successful acceleration of  $N^{5+}$  ( $A/q=2.8$ ) beam to the designed energy of 1.8 MeV/u. With this test, the complete validation of HCI design has been successfully accomplished. Further, the process of next beam tests in HCI for higher  $A/q$  is underway. The procurement of components required to commission and integrate the HCI to SC-LINAC is also under process. Figure 1 shows the present status of the HCI facility.

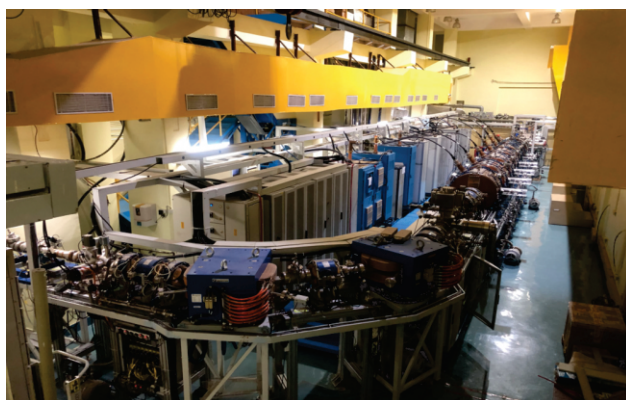


Figure 1: High Current Injector Accelerator Facility.

#### 2.1.2 ECR ion source

G Rodrigues, P S Lakshmy, Sarvesh Kumar, Kedar Mal, R Ahuja, Y Mathur, R K Gurjar and Mukesh Kumar

##### (A) Performance of 18 GHz High Temperature Superconducting (HTS) ECR ion source

In this academic year, activities connected to the development of metal beams continued using the sputtering system. A motorized sputtering system with a Wilson seal arrangement was installed onto the injection side of the source as shown in Figure 2 (a). A copper wire of diameter 4mm was fixed at the end of the sputtering rod. The sputtering location with respect to the injection field maxima can be tuned by moving the sputtering rod in and out. The sputtering voltage has been enhanced and can be ramped up to -2 kV. A 24V, 2A rated power supply was installed on the 30kV platform and was powered by a 3 kV isolation transformer to operate the sputtering unit. The remote operation of the sputtering motor was looked into in detail for ease of operation and was tested successfully.

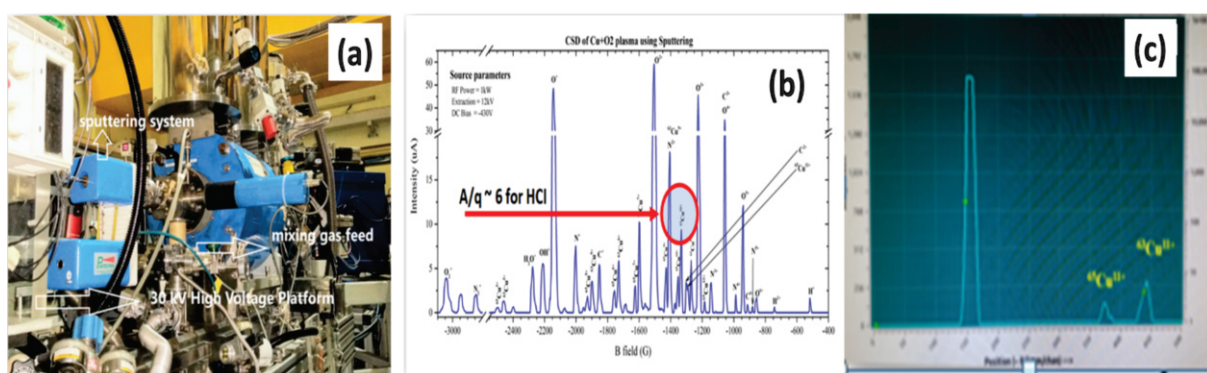


Figure 2 (a): Sputtering system coupled at the injection side of the ECR source, (b) CSD spectrum of Cu plasma using  $O_2$  as mixing gas, (c) Beam profile showing isotopes of Cu.

The tuning of various charge states of Cu beams were carried out with the mixing of different gases, like  $O_2$ , Ar and Ne. In Figure 2(b), a charge state distribution (CSD) spectrum of Cu plasma with  $O_2$  as the mixing gas is shown after optimizing for  $Cu^{6+}$ . The spectrum clearly shows two isotopes of Cu i.e.,  $^{63}Cu$  and  $^{65}Cu$ , getting populated. Figure 2(c) depicts the beam profiles of Cu isotopes. During continuous operation, it has been observed that the RF power losses have been extremely large and getting lost much before reaching the ECR plasma. A detailed analysis was carried out to compare the performance of the source in terms of the extracted beam intensities and the x-ray radiation levels using Ne and Ar beams. This comparative analysis showed that only half of the Klystron power was getting absorbed in the plasma. A detailed modelling of the RF coupling to the load will be carried out to identify the location of the RF power losses.

**(B) Beam acceleration tests for energy validation of DTL cavities**

Beam acceleration tests through RFQ and DTL accelerators were carried out systematically using beams of  $A/q = 2.8$ . All the beam tests have been carried out using  $N^{5+}$  since this beam was used earlier for the energy validation of the first and second DTL cavities. The verification of the energy gain of DTL3, DTL4, DTL5 and DTL6 were each carried out separately. The boosted energy achieved from DTL3 to DTL 6 cavities are 11.9MeV, 16.1 MeV, 20.4 MeV and 25.2 MeV respectively. Beam tuning optimisation was carried out by iterative transverse and longitudinal beam tuning for each of the DTL cavities in a progressive manner. The bunch width was optimized using 12.125 MHz, MHB and the 48.5 MHz, spiral bunchers. Figure 3 shows the beam profile of the accelerated  $N^{5+}$  beam in the MEBT section. Test runs have also been carried out successfully after shifting the remote-control operation to the Pelletron control room.

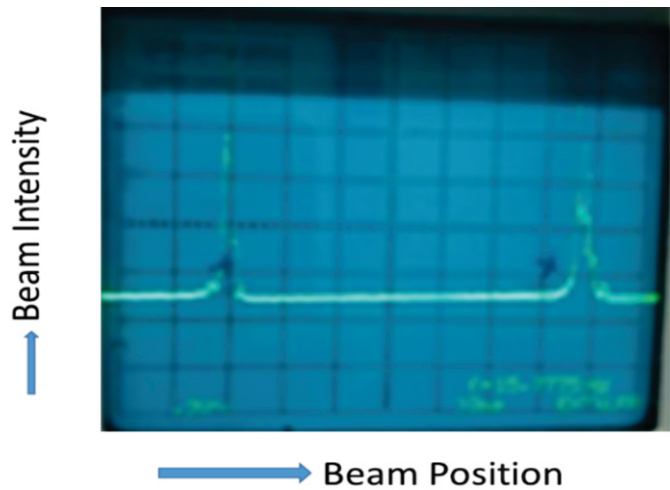


Figure 3: Beam profiles in HEBT section.

**(C) Design and fabrication of a 40kV high voltage platform**

A 40 kV High Voltage platform has been designed and fabricated in order to upgrade the existing 30 kV High Voltage platform for handling more equipment which are required to be operated at source potential, viz, gas needle valves, gas bottles, power supplies etc. Additionally, the increased voltage will allow to improve the extraction conditions and also for better beam stability. The newly designed model is shown in Figure 4. The high voltage platform which will be biased to 40 kV with respect to the 200 kV High Voltage platform will house various kinds of power supplies required for DC bias, sputtering system and micro oven system, besides using gas bottles, needle valves etc. at the same source potential. It is expected that a substantial improvement of beam transmission will be achieved by operating at voltages above 25 kV. The fabrication of the structure has been completed and presently finer finishings are being carried out.

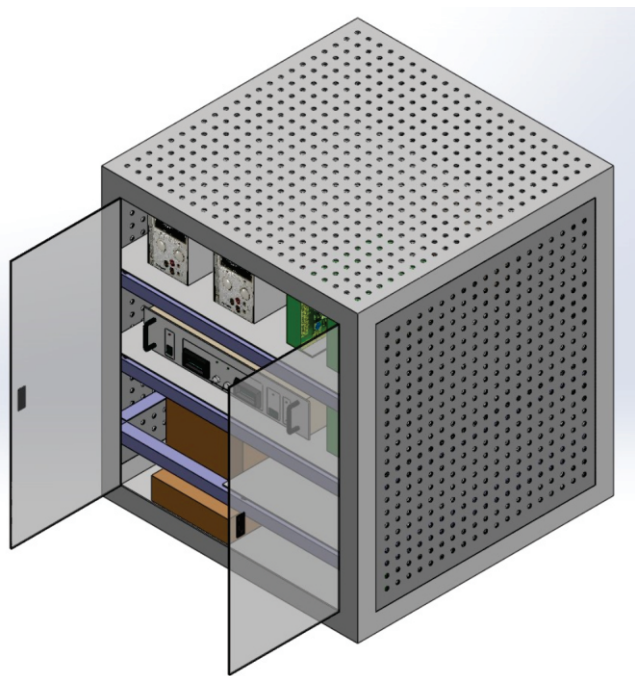


Figure 4: Model of the 40 kV High Voltage Platform.

**(D) High voltage power supplies of HTS ECRIS and LEBT****(i) Preventive maintenance schedule & breakdown maintenance**

Yearly scheduled preventive maintenance of every instrument is performed to preserve its life, improve its performance and to ensure breakdown-free operation during the year-long continuous operation of the system. In ion source area, all high voltage power supplies (HVPS), viz., 200 kV HVPS, Extractor & Focus HVPS have been cleaned and all the loose connections were checked & finally tested and operated by remote control. Besides this, bleeders were cleaned and covered with acrylic sheet. DC bias power supply (-1kV) was found faulty due to a suspected discharge/spark. It was replaced by -10 kV high voltage power supply. Tripping problem in the high temperature superconducting magnet power supply (HTS-MPS) was arising due to voltage tap signals coming from the HTS magnets. This was finally repaired & maintenance was carried out. In figure 5, 200 kV high voltage platform power supply, HTS magnet power supply & electronics modules of the HTS-MPS are shown.

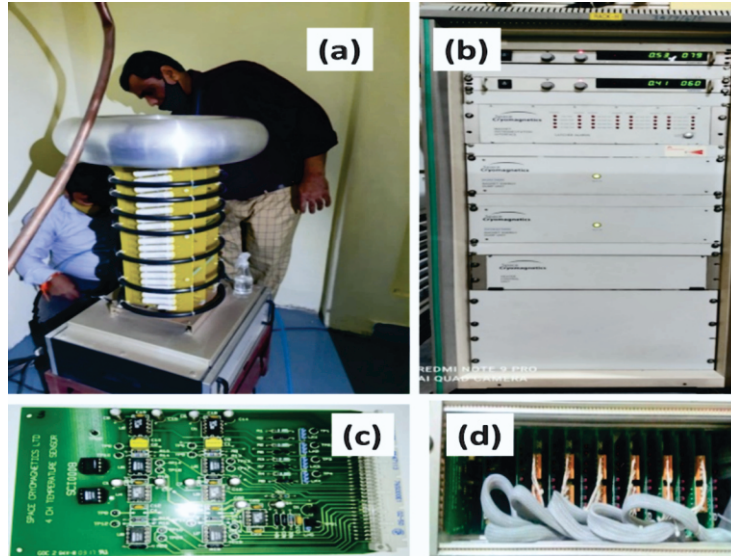


Figure 5: (a) 200 kV High Voltage Platform power supply, (b) HTS magnet power supply, and (c & d) Electronics modules of HTS-MPS.

**(ii) Development Activities: Sputtering Motor Controller (SMC) for metal beam development**

Sputtering Motor Controller (SMC) was developed in-house and utilized for forward and backward motion (In or Out mode) of the sample to be sputtered for development of metal ion beams. This unit was successfully installed on the 30kV high voltage platform. A block diagram of the SMC is shown in Figure 6.

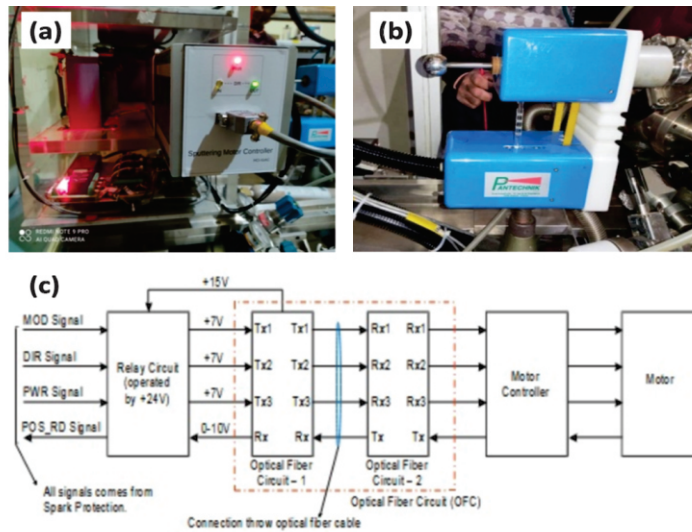


Figure 6. Detailed view of SMC and its associated block diagram.

**(E) Study and improvements of a radially coupled coaxial fast Faraday cup design**

For charge profile measurements of short bunches ( $\leq 5$  ns), the impedance matching of the Faraday cup structure is critical to avoid signal reflections. The Fast Faraday cups (FFCs) are thus a variant of Faraday cups used to measure fast beam signals like the short beam bunches. A typical coaxial FFC design is based on a tapered matching of the impedance of the  $50 \Omega$  co-axial transmission line to the wave impedance. The beam is axially stopped on to the central conductor of the co-axial cable. Meanwhile, alternate FFC designs based on radial coupling in the central



conductor and microstrip based designs have been used in various accelerator facilities. So far, most studies available in literature on FFCs are focused on impedance mismatch aspects. We modified the design of radially-coupled coaxial FFC (RCFFC; built by Fermi Research Alliance, LLC) for beam conditions at the High Current Injector (HCI). Due to the narrow beam limiting aperture of 0.8 mm, the primary drawback of the original design was the low signal to noise ratio, and a need for precise beam alignment with long averaging times for the measurement. We have increased the aperture and used a transition method without curved structures to induce an improved signal to noise ratio. It was done for the transition from N-type connector to the cup region to achieve uniform impedance and low reflection. Figure 7 shows the cross-sectional view of the model of the RCFFC simulated using CST Microwave Studio.

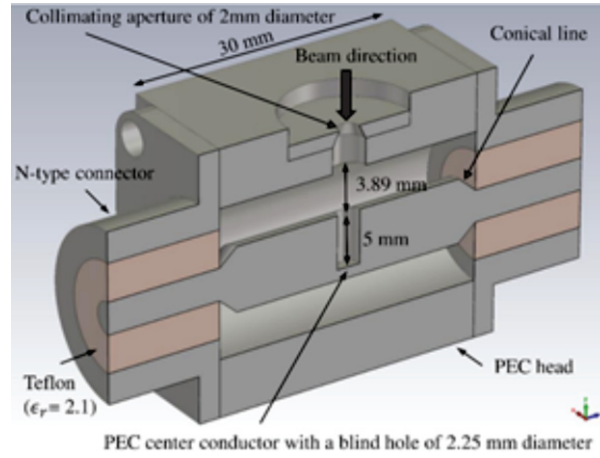


Figure 7: Model (cross-sectional view) of the RCFFC simulated using CST Microwave Studio.

The simulated return loss, insertion loss and the characteristic impedance of the optimized geometry of RCFFC are shown in Figure 8. From Figure 8 (b), it can be seen that the impedance difference between the conical and coaxial lines is almost equal to  $50\ \Omega$ .

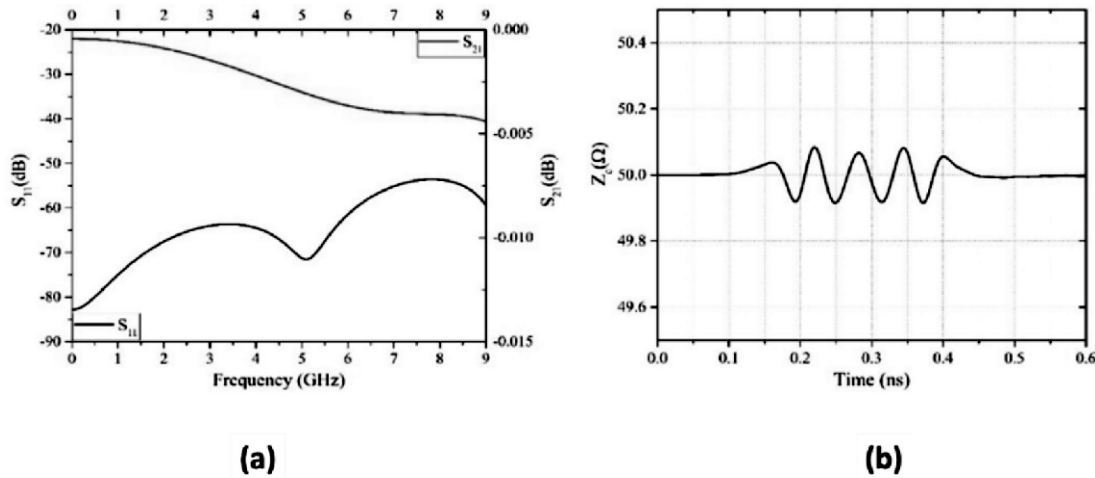


Figure 8: Simulated results: (a) Return loss at the input port, and insertion loss between two ports, (b) characteristic impedance ( $Z_0$ ).

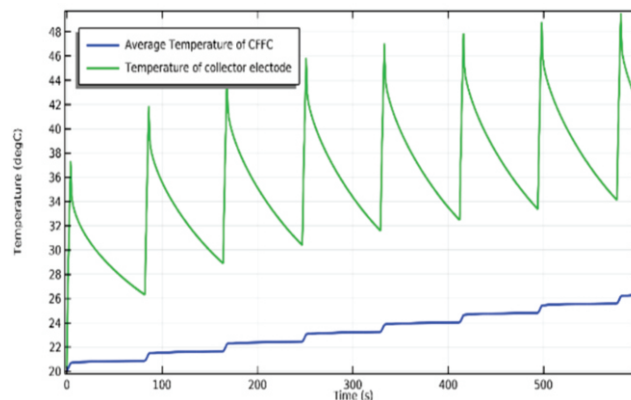


Figure 9. Evolution of temperature with pulsed beam, modelled using COMSOL Multi-Physics. Beam parameters:  $A/q=6$ , beam intensity =  $1\ \mu\text{A}$ , pulse width =  $4\text{s}$ , duty cycle =  $4.85\ \%$ .



The thermal study of the RCFFC for the pulsed beam has been carried out using COMSOL Multi-Physics. In the HCI, a multi harmonic buncher (operating at a fundamental frequency 12.125 MHz) generates the bunched beam with a bunch length in the order of few ns. Considering a worst-case scenario of 4 ns, the duty cycle of the pulse would be 4.85 %. This in turn implies that the thermal load in the RCFFC will be active only for 4ns out of 82.47ns (time period of one pulse).

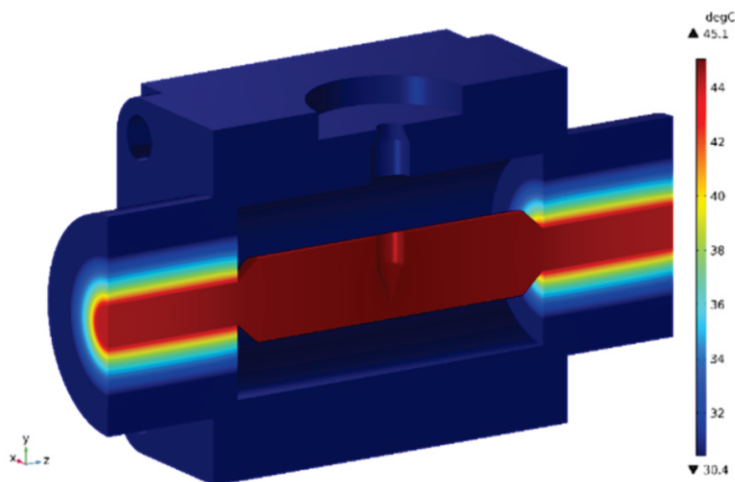


Figure 10. Temperature distribution of the CFCC with pulsed beam, modelled using COMSOL Multi-Physics. Beam parameters are  $A/q=6$ , current = 1  $\mu\text{A}$ , pulse width = 4s, duty cycle= 4.85 %.

In the simulation, the step size should be less than the width of the pulse, otherwise the thermal load would not be activated. To simulate the RCFFC for thermal analysis using the pulse of width 4ns with duty cycle 4.85 % and step size 1ns, the total number of steps from 0 to 10 minutes would be 6E11. It is thus impossible to handle such large number of steps for modelling on a normal computer having 16 GHz RAM using 4 cores. Therefore, we have tried to use the frequency 12.125 millihertz instead of 12.125 MHz to reduce the total number of steps in the simulation. Therefore, the pulse width now becomes 4 s and the total number of steps would be 600 for a time interval from 0 to 10 minutes. The evolution of the temperature of the collector electrode and average temperature of the RCFFC for a bunched beam having  $A/q = 6$  is shown in Figure 9. The temperature distribution of the RCFFC for a bunched beam is shown in Figure 10. It is observed that the maximum temperature of the collector electrode reaches about 50°C and maximum average temperature of the RCFFC is 27°C. These temperature values are much below the melting point of Teflon (327°C) and therefore no active cooling is actually required in the RCFFC. The study of signal induction, field dilution, and secondary electron emission aspects are presently ongoing.

### 2.1.3 Multi-harmonic buncher (MHB)

A Sarkar, Sarvesh Kumar, VV V Satyanarayana, RAhuja, Y Mathur, Parmanand Singh, S Venkataramanan

The 12.125 MHz MHB has been operational from the last six years to provide bunched beams of the order of few ns at the entrance of RFQ in HCI. The bunch length of the beam is measured using Fast Faraday Cups (FFC) installed before RFQ and at the entrance of DTL#1 cavity. The first FFC is a commercial, coaxial type, and second FFC is a stripline type, obtained on loan from BARC Mumbai. The  $\text{N}^{5+}$  beam of 8 keV/u energy is bunched to 2 ns FWHM at the RFQ entrance and is further accelerated through RFQ. The beam is further transported to MEBT section of HCI and a spiral buncher at the DTL entrance re-bunches it for the next stage of acceleration. The longitudinal emittance can be generally measured anywhere in the beamline if the diagnostic tools to measure the bunch width are available. A voltage scan on MHB was done to obtain varying bunch widths measurable at the available FFCs along the beamline. The longitudinal emittance value was extracted from this data. Further analysis is going on with the available data.

### 2.1.4 Radio frequency quadrupole

Sugam Kumar, R. Ahuja, C.P. Safvan

#### (A) Beam acceleration through radio frequency quadrupole (RFQ)

Beam acceleration test was carried out this year by injecting  $\text{N}^{5+}$  beam of energy 8 keV/u into RFQ as well as through all DTLs. To maximize the beam current just after the DTL cavities, the phase and amplitude of all cavities (MHB, RFQ, SB and DTLs) were optimized. After optimization of the phase and amplitude of the RF cavities, the beam intensity was increased further from 300 enA to 1.4  $\mu\text{A}$  at the exit of the DTL#4 cavity. The final beam intensity of  $\text{N}^{5+}$  beam through DTL#6 was achieved with more than 150enA at the required energy of 1.8 MeV/u. The beam energy has been confirmed through the Achromat magnetic field of 6264.7 Gauss. The various beam and RF parameters of RFQ and DTLs are listed in Table 1.